Unusual Solid-state Reaction of $[\{CrL(acac)\}_2(\mu\text{-}H_3O_2)][PF_6]_3$. Isolation and Crystal Structures of $[CrL(acac)F]PF_6$ and $[CrL(acac)(O_2PF_2)]PF_6$ (L = 1,4,7-trimethyl-1,4,7-triazacyclononane, acac = pentane-2,4-dionate)†

Ursula Bossek,[a] Gabriele Haselhorst,[a] Sylvia Ross,[a] Karl Wieghardt*,[a] **and Bernhard Nuber**[b]

[a] *Lehrstuhl für Anorganische Chemie I, Ruhr-Universität, D-44780 Bochum, Germany*

[b] *Anorganisch-Chemisches Institut der Universität, Im Neuenheimer Feld 270, D-69120 Heidelberg, Germany*

From a concentrated aqueous solution of the mononuclear complexes $[CrL(acac)(OH)]PF_6\cdot H_2O$ and $[CrL(acac)(OH_2)][ClO_4]_2$ at pH ≈ 6 the dinuclear $H_3O_2^-$-bridged species $[\{CrL(acac)\}_2(\mu\text{-}H_3O_2)][PF_6]_3$ was isolated as a crystalline red solid (L = 1,4,7-trimethyl-1,4,7-triazacyclononane, acac = pentane-2,4-dionate). The dinuclear complex reacted at 145 °C in the solid state with evolution of 3 equivalents of HF, yielding quantitatively the mononuclear complexes $[CrL(acac)F]PF_6$ and $[CrL(acac)(O_2PF_2)]PF_6$ in equal amounts. Thus an unco-ordinated PF_6^- anion is thermally converted into a co-ordinated fluoride and a monodentate $O_2PF_2^-$ ligand. The crystal structures of $[CrL(acac)(OH_2)][ClO_4]_2$, $[CrL(acac)F]PF_6$ and $[CrL(acac)(O_2PF_2)]PF_6$ have been determined by X-ray crystallography. The cobalt(III) complex $[\{CoL(acac)\}_2(\mu\text{-}H_3O_2)][PF_6]_3$ has also been prepared and structurally characterized. It is isostructural with the chromium analogue. Heating to its melting point at 190 °C did not induce solid-state transformation to mononuclear cobalt(III) species analogous to $[CrL(acac)F]PF_6$ and $[CrL(acac)(O_2PF_2)]PF_6$.

Ardon and Bino[1] have in a series of elegant papers shown that the classic 'olation' reaction, *i.e.* formation of μ-hydroxo-bridged chromium(III) and cobalt(III) complexes, proceeds *via* hydroxoaqua-bridged dinuclear precursors, equation (1)

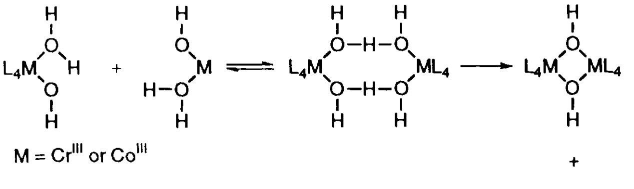

(1)

(L = amine). Subsequently, many complexes containing one or two such (μ-H_3O_2) bridges have been isolated as crystalline solids and their structures firmly established by X-ray crystallography. The $H_3O_2^-$ bridge contains a very strong O–H–O hydrogen bond (O ••• O ≈ 2.41–2.46 Å) which may be symmetric or asymmetric O–H ••• O. One of the puzzling aspects of their work has been the observation that reaction (1) proceeds smoothly in solution and in some cases even in the solid state upon heating of the sample only if two (μ-H_3O_2) bridges are present which are positioned *cis* to each other.[1,2] Dinuclear complexes with only one $H_3O_2^-$ bridge or polynuclear chain structures with two mutually *trans* $H_3O_2^-$ bridges do in general not lead to hydroxo-bridged species. Thus reaction (2) is not of the general type. A possible exception to this observation is Springborg's iridium complex[3] *cis*-$[\{Ir(en)_2\}_2(\mu\text{-}OH)(\mu\text{-}H_3O_2)]^{4+}$ (en = ethane-1,2-diamine) which contains one μ-hydroxo and in *cis*-position a $H_3O_2^-$ bridge and is readily intramolecularly converted into the di-μ-hydroxo species $[\{Ir(en)_2\}_2(\mu\text{-}OH)_2]^{4+}$.

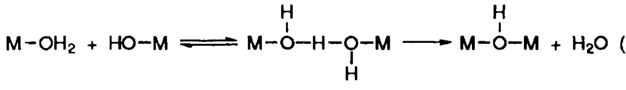

$$M{-}OH_2 + HO{-}M \rightleftharpoons M{-}\overset{H}{O}{-}H{-}\underset{H}{O}{-}M \longrightarrow M{-}\overset{H}{O}{-}M + H_2O \quad (2)$$

We have recently isolated and structurally characterized two dinuclear complexes each containing only one $H_3O_2^-$ bridge, namely $[\{Cr^{III}L(acac)\}_2(\mu\text{-}H_3O_2)][PF_6]_3$[4] and $[\{Ru^{III}L(acac)\}_2(\mu\text{-}H_3O_2)][PF_6]_3$[5] where L represents the cyclic triamine 1,4,7-trimethyl-1,4,7-triazacyclononane and acac is pentane-2,4-dionate. In addition, the isostructural mononuclear species $[RuL(acac)(OH)]PF_6\cdot H_2O$ and $[CrL(acac)(OH)]PF_6\cdot H_2O$ have also been structurally characterized.[4,5] Heating a solid sample of $[RuL(acac)(OH)]PF_6\cdot H_2O$ *in vacuo* to 130 °C for 8 h yielded the μ-oxo-diruthenium(III) species $[\{RuL(acac)\}_2(\mu\text{-}O)][PF_6]_2$. This is an interesting solid-state reaction because the mononuclear precursor does not contain a terminal RuOH group but a $Ru^{III}(O_2H_3)$ moiety with a terminally bound $H_3O_2^-$ ligand. Thus reaction (3) occurs. In the corresponding

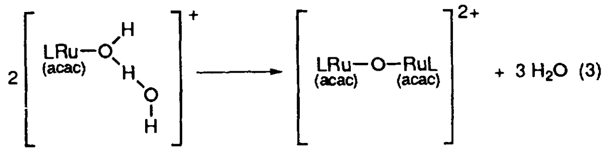

(3)

chromium(III) complex $[CrL(acac)(OH)]PF_6\cdot H_2O$ the O–H ••• O interaction between CrOH and a water molecule is weaker. Heating of this species does not lead to the $[\{CrL(acac)\}_2(\mu\text{-}O)]^{2+}$ analogue. Thus reaction (3) does not occur analogously.

Considering this diverse reactivity of analogous octahedral transition-metal complexes with one terminal or bridging

---

† *Supplementary data available:* see Instructions for Authors, *J. Chem. Soc., Dalton Trans.*, 1994, Issue 1, pp. xxiii–xxviii.

$H_3O_2^-$ ligand, we decided to investigate the reactivity of such complexes of chromium(III) and cobalt(III) in further detail. Here we report the unusual behaviour of solid $[\{Cr^{III}L(acac)\}_2(\mu\text{-}H_3O_2)][PF_6]_3$ and its cobalt(III) analogue on heating.

Results

Syntheses of Complexes.—Scheme 1 summarizes the synthetic routes to complexes **1**–**7**. Previously we have reported[4] that the reaction of $[CrLBr_3]$ or, as we found now, of $[CrLCl_3]$ **1** with an excess of sodium pentane-2,4-dionate Na[acac] in aqueous solution at 70–80 °C yields, after addition of KPF_6, red crystalline $[CrL(acac)(OH)]PF_6 \cdot H_2O$ **2**. When the above red solution was adjusted to pH 5–6 with HPF_6 red crystals of $[\{CrL(acac)\}_2(\mu\text{-}H_3O_2)][PF_6]_3$ **4** precipitated. The structures of both **2** and **4** have been determined by X-ray crystallography.[4] When the above red solution was adjusted to pH 1 by using concentrated $HClO_4$ and solid $NaClO_4$ was added, red crystals of $[CrL(acac)(OH_2)][ClO_4]_2$ **3** were obtained. The mononuclear octahedral nature of the dication was established by X-ray crystallography (see below).

Heating of a solid sample of complex **4** *in vacuo* at 160 °C for 4 h produced a deep red residue which dissolved readily in water. When such a solution was adjusted to pH 9 by addition of NaOH and allowed to stand at ambient temperature in an open vessel for 2–3 d red crystals of $[CrL(acac)F]PF_6$ **5** formed in 33% yield based on the total chromium(III) content. If, on the other hand, the pH was adjusted to 5 by using aqueous HPF_6 the same procedure produced red crystals of $[CrL(acac)(O_2PF_2)]PF_6$ **6** also in ≈33% yield.

Investigation of this solid-state reaction of complex **4** by thermal gravimetry and differential thermogravimetry showed that the sample lost 1.76% weight in a single step at 145 °C (peak maximum of the DTA experiment). Qualitatively and quantitatively we established that HF is the sole gaseous product. The observed weight loss corresponds then exactly to 3 equivalents of HF per dinuclear complex **4** which produces equal amounts of **5** and **6** [equation (4)].

$$[\{CrL(acac)\}_2(\mu\text{-}H_3O_2)][PF_6]_3 \xrightarrow[-2HF]{145\,^{\circ}C} [CrL(acac)F]PF_6 + [CrL(acac)(O_2PF_2)]PF_6 \quad (4)$$

Fast atom bombardment (FAB) mass spectrometry of complex **4** and of the solid residue of its solid-state reaction proved to be particularly informative. The spectrum of **4** displays a weak peak (< 1%) at m/z = 969.3 which shows the correct isotope distribution for chromium and is assigned to $[\{CrL(acac)\}_2(\mu\text{-}H_3O_2)(PF_6)_2]^+$. The base peak at m/z = 339.2 corresponds to $[CrL(acac)(OH)]^+$. Fig. 1 shows the interesting FAB spectrum of the residue obtained after heating of **4** *in vacuo* at 160 °C for 4 h. Two prominent peaks at m/z = 423 and 341 (relative intensity 87 and 100%, respectively) correspond to the calculated masses of the ions $[CrL(acac)F]^+$ and $[CrL(acac)(O_2PF_2)]^+$, respectively. In addition, three weak (< 1%) cluster-ion peaks of nearly equal intensity are observed at m/z = 827, 909 and 991 which correspond to $[\{CrL(acac)F\}_2(PF_6)]^+$, $[\{CrL(acac)F\}\{CrL(acac)(O_2PF_2)\}(PF_6)]^+$ and $[CrL(acac)(O_2PF_2)_2(PF_6)]^+$. Since the three clusters are formed in about equal quantities in the statistical ratio 1 : 1 : 1, complexes **5** and **6** are considered to be the sole reaction products (ratio 1 : 1). We feel that this distribution rules out any significant build-up of the dinuclear species **A** with an *O,O′*-bridging $O_2PF_3^{2-}$ ligand which might be considered to be an intermediate in the thermal transformation of one PF_6^- anion into an $O_2PF_3^{2-}$ ligand. Note that the molecular-ion peak of this intermediate would have the same mass as that of the cluster $[\{CrL(acac)F\}\{CrL(acac)(O_2PF_2)\}(PF_6)]^+$ but it would not account for the other two cluster peaks.

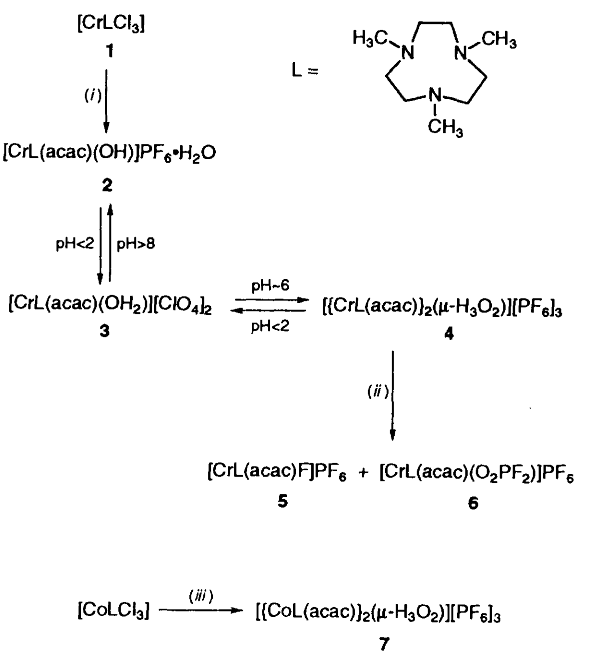

Scheme 1 Reaction conditions: (*i*) Na[acac], H_2O, pH 9; (*ii*) 4 h of heating at 160 °C *in vacuo*; (*iii*) Na[acac], H_2O, pH 6

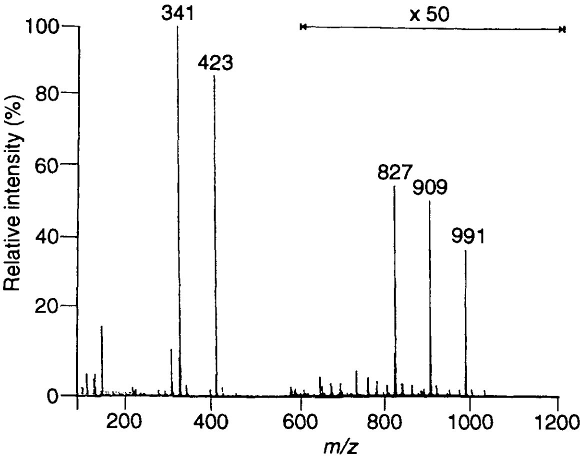

Fig. 1 Fast atom bombardment mass spectrum of complex **4** after treatment *in vacuo* at 160 °C for 4 h

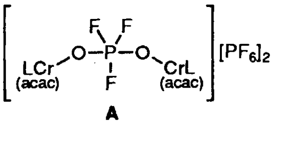

A

When a reaction mixture of $[CoLCl_3] \cdot H_2O$* and Na[acac] in water was heated to 70 °C until a clear red solution resulted, red-violet crystals of $[\{CoL(acac)\}_2(\mu\text{-}H_3O_2)][PF_6]_3$ **7** precipitated upon addition of $NaPF_6$. The crystal structure determination established that **7** is isostructural with complex **4** (see below). Even the crystal packing is very similar (Fig. 5). Thermogravimetric experiments showed that **7** does not react with evolution of HF up to a heating temperature of 240 °C. It melts at 190 °C without loss of weight. This is an unexpected

---

* The synthesis of $[CoL'Cl_3]$ where L′ = 1,4,7-triazacyclononane has been described in detail;[6] $[CoLCl_3] \cdot H_2O$ has been prepared similarly (see Experimental section).

Table 1 The UV/VIS spectral and magnetic data for the complexes

Complex	λ_{max}/nm (ε/dm^3 mol^{-1} cm^{-1})^a	λ_{max} (reflectance spectrum)/nm	μ_{eff}(298 K)/μ_B
2	525 (78), 420 (sh), 304 (2022), 246 (1926)	518	3.79
3	513 (65), 415 (sh), 375 (sh), 317 (2406), 247 (2318)	504	3.82
4	515 (104), 415 (sh)	496	See ref. 4^b
5	562 (74), 387 (244), 322 (2205), 244 (2581)	n. m.^{c}	3.69
6	533 (67), 331 (4396), 232 (5095)	n. m.	3.93
7	537 (100), 422 (sh), 319 (4060), 275 (7854)	n. m.	Diamagnetic

^{a} Solvent: Me$_3$CN. ^{b} The chromium ions are weakly antiferromagnetically coupled. ^{c} n. m. = Not measured.

result considering the structural similarity of **4** and **7**. The FAB mass spectrum displays the 100% peak at *m/z* = 329.2 which corresponds to $[\mathrm{CoL(acac)}]^+$ and a peak at *m/z* 693.3 (0.8%) due to $[\{\mathrm{CoL(acac)}\}_2(\mathrm{H_3O_2})]^+$.

Spectroscopic Characterization of the Complexes.—In the infrared spectrum of complex **6** moderately strong bands at 1315, 1145 and 1150 cm^{-1} are assigned to the ν(P=O) stretching frequencies of the monodentate $\mathrm{O_2PF_2^-}$ ligand. A band at 796 cm^{-1} is tentatively assigned to the $\nu_{sym}(\mathrm{PF_2})$ stretching mode; the corresponding $\nu_{asym}(\mathrm{PF_2})$ mode at higher energy is probably hidden under the $\nu(\mathrm{PF_6})$ stretching mode at 830 cm^{-1}. We refrain from a more detailed comparison of these data with those reported for $\mathrm{Cr(O_2PF_2)_3{\cdot}HPO_2F_2}$[7a] or $\mathrm{Cr(O_2PF_2)_3}$[7b] where the ligand is proposed to be didentate or for the salt $\mathrm{K[O_2PF_2]}$.[8,9]

Table 1 summarizes electronic spectral and magnetic data for complexes **2**–**7**. The lowest energy transition $^4A_{2g} \longrightarrow {}^4T_{2g}$ (in O_h symmetry) in the visible region allows an estimate of the strength of the ligand field. Since all complexes under investigation contain the Cr^{III}L(acac) fragment, variations of this absorption maximum are primarily due to a differing ligand-field strength of the sixth ligand X. Since the solution spectra of **2**–**4** may involve protonation–deprotonation and/or association–dissociation equilibria we also measured the solid-state reflectance spectra. From these data it is clear that the usual spectrochemical series $\mathrm{F^-} < \mathrm{OH^-} < \mathrm{H_2O}$ arranged in order of increasing 10*Dq* is retained in the present series. Note that **2** does not contain a real terminal hydroxo but a hydroxoaqua ligand, at least in the solid state. The ligand $\mathrm{O_2PF_2^-}$ is weaker than $\mathrm{^-OH(H_2O)}$ but stronger than $\mathrm{F^-}$ and the μ-$\mathrm{H_3O_2^-}$ bridge exerts the strongest ligand field in the series.

Description of Crystal Structures.—The structures of the hydroxo species **2** and the (μ-$\mathrm{H_3O_2}$) bridged complex **4** have been reported previously.[4] The mononuclear cations of the aqua species in crystals of complex **3**, the fluoro complex in **5** and of the difluorophosphato complex in **6** are shown in Figs. 2, 3 and 4 respectively. Table 2 summarizes selected bond distances and angles.

All these compounds contain a Cr^{III}L(acac) fragment with a facially co-ordinated cyclic triamine and a didentate *O,O′*-co-ordinated pentane-2,4-dionate ligand. The metric details of this fragment are within experimental error identical for all complexes including those reported for **2** and **4**. The average Cr–N distance is 2.100 Å and the average Cr–O$_{acac}$ is 1.938 Å. The dimensions of the Cr(acac) fragment are also virtually identical in all these compounds. They agree well with those reported for [Cr(acac)$_3$].[10] Only the Cr–X distances of the sixth ligand vary (Table 2): the Cr–OH distance in **2** is 1.90(2) Å, the Cr–OH$_2$ bond in **3** is as expected significantly longer at 2.067(6) Å, whereas the Cr–O bond length of the $\mathrm{H_3O_2^-}$ bridge in **4** is intermediate between these two Cr–O distances [1.969(4) Å]. It should be noted that the hydroxo ligand in **2** forms an OH⋯O bonding contact to a water molecule of crystallization.[4] The O⋯O distance is 2.66(3) Å which indicates a weaker hydrogen bond than is observed in the μ-$\mathrm{H_3O_2^-}$ bridge in **4** [2.496(6) Å] for which a symmetrical O⋯H⋯O hydrogen bond has been reported.[4]

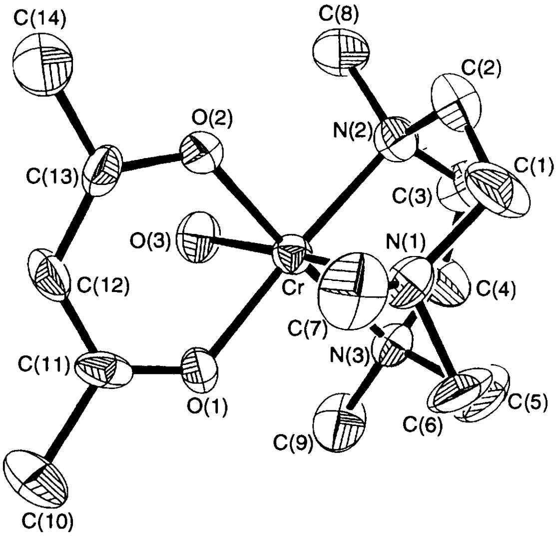

Fig. 2 Structure of the dication $[\mathrm{CrL(acac)(OH_2)}]^{2+}$ in crystals of complex **3**

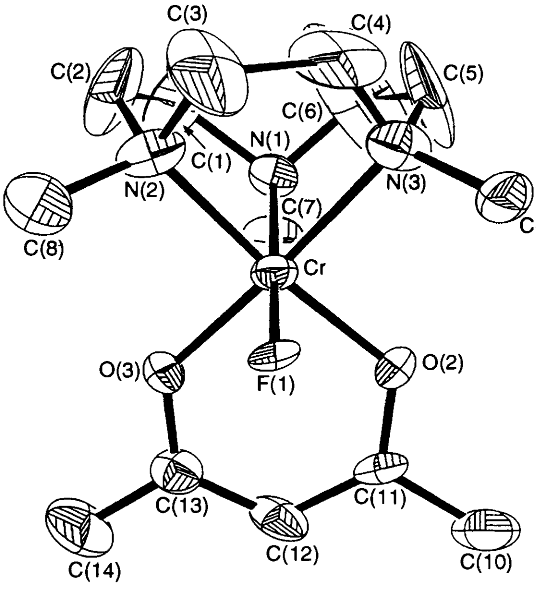

Fig. 3 Structure of the monocation $[\mathrm{CrL(acac)F}]^+$ in crystals of complex **5**

Fig. 4 shows the structure of the mononuclear cation in crystals of complex **6**. It lies on a crystallographic mirror plane which is not compatible with λλλ (or δδδ) conformation of the three five-membered chelate rings Cr–N–C–C–N of the co-ordinated cyclic triamine. Consequently, the two carbon atoms C(1) and C(1a) are disordered. It has not been possible to model this disorder satisfactorily by a split-atom model.

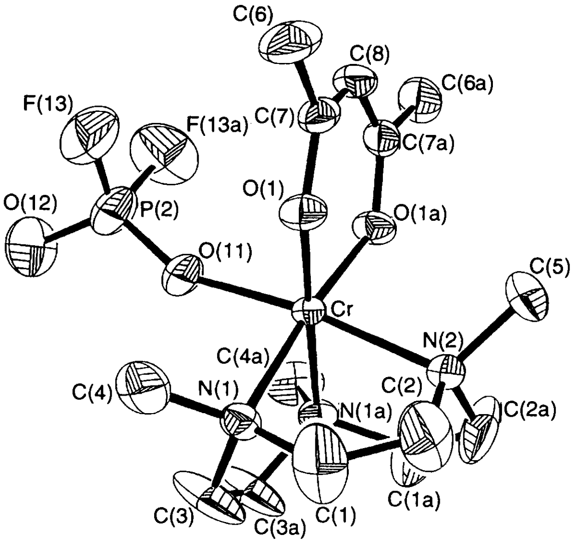

Fig. 4 Structure of the monocation $[CrL(acac)(O_2PF_2)]^+$ in crystals of complex **6**

Table 2 Selected bond lengths (Å) and angles (°) for complexes **3** and **5**–**7**

Complex **3**			
Cr–N(1)	2.016(8)	Cr–O(1)	1.917(8)
Cr–N(2)	2.098(10)	Cr–O(2)	1.946(8)
Cr–N(3)	2.104(9)	Cr–O(3)	2.067(6)
N(2)–Cr–N(1)	85.1(4)	O(3)–Cr–N(2)	94.9(3)
N(3)–Cr–N(1)	84.7(3)	O(1)–Cr–N(3)	93.6(3)
O(1)–Cr–N(1)	93.7(3)	O(2)–Cr–N(3)	174.9(3)
O(2)–Cr–N(1)	93.4(3)	O(3)–Cr–N(3)	91.5(3)
O(3)–Cr–N(1)	176.2(3)	O(2)–Cr–O(1)	91.3(3)
N(3)–Cr–N(2)	83.1(4)	O(3)–Cr–O(1)	86.0(3)
O(1)–Cr–N(2)	176.6(3)	O(3)–Cr–O(2)	90.4(3)
O(2)–Cr–N(2)	92.0(3)		
Complex **5**			
Cr–N(1)	2.122(9)	Cr–N(2)	2.043(13)
Cr–N(3)	2.111(13)	Cr–F(1)	1.864(6)
Cr–O(2)	1.993(9)	Cr–O(3)	1.929(9)
Complex **6**			
Cr–N(1)	2.096(4)	Cr–O(11)	1.964(5)
Cr–N(2)	2.099(6)	P(2)–O(11)	1.453(5)
Cr–O(1)	1.925(3)	P(2)–O(12)	1.436(8)
P(2)–F(13)	1.518(5)		
O(11)–P(2)–O(12)	117.9(4)	O(11)–P(2)–F(13a)	107.8(2)
O(11)–P(2)–F(13)	107.8(2)	F(13)–P(2)–F(13a)	100.4(4)
O(12)–P(2)–F(13)	110.8(3)	Cr(1)–O(11)–P(2)	154.3(4)
Complex **7**			
Co(1)–O(1)	1.884(2)	Co(1)–O(2)	1.882(2)
Co(1)–O(3)	1.931(3)	Co(1)–N(1)	1.995(3)
Co(1)–N(2)	1.977(3)	Co(1)–N(3)	1.982(3)
O(1)–Co(1)–O(2)	94.9(1)	O(1)–Co(1)–O(3)	88.0(1)
O(2)–Co(1)–O(3)	88.9(1)	O(1)–Co(1)–N(1)	175.6(1)
O(2)–Co(1)–N(1)	87.6(1)	O(3)–Co(1)–N(1)	95.6(1)
O(1)–Co(1)–N(2)	89.4(1)	O(2)–Co(1)–N(2)	93.9(1)
O(3)–Co(1)–N(2)	176.2(1)	N(1)–Co(1)–N(2)	86.9(1)
O(1)–Co(1)–N(3)	91.3(1)	O(2)–Co(1)–N(3)	173.7(1)
O(3)–Co(1)–N(3)	90.2(1)	N(1)–Co(1)–N(3)	86.2(1)
N(2)–Co(1)–N(3)	87.2(1)		

The $O_2PF_2^-$ anion is clearly bound to chromium in a monodentate fashion *via* one of the oxygen atoms. It possesses crystallographic site symmetry *m*. Two different P–O bond lengths are observed: a short terminal P=O bond [1.436(8) Å] and a longer distance [1.453(5) Å] of the metal-bound P–O group. The two P–F bond lengths are equivalent at 1.518(5) Å. These distances may be compared with those reported for alkali-metal salts of the $O_2PF_2^-$ anion (C_{2v} symmetry): P=O 1.47, P–F 1.575 Å.[9] The F–P–F and O–P–O bond angles are also quite different in complex **6** and in the unco-ordinated anion: 100.4(4) and 117.9(4)°; $K[O_2PF_2]$, 97.1 and 122.4, respectively. For $Cr(O_2PF_2)_3{\cdot}HPO_2F_2$ and $Cr(O_2PF_2)_3$ it has been suggested that the three $PO_2F_2^-$ anions are co-ordinated in a didentate *O,O'* fashion.[7] To the best of our knowledge **6** represents the first structurally characterized complex containing a monodentate difluorophosphate anion.

Fig. 5 displays the structure of the dinuclear trication in crystals of complex **7**; it possesses crystallographic symmetry C_i. Since the hydrogen atoms of the $H_3O_2^-$ bridge have been located and successfully refined in the crystal-structure determination it is possible to discuss geometrical details of the $Co(\mu\text{-}H_3O_2)Co$ core (Table 3) and compare them with those in the chromium(III) analogue **4**[4] and in $[\{RuL(acac)\}_2(\mu\text{-}H_3O_2)][PF_6]_3$.[5] It is noteworthy that all three compounds crystallize in the same triclinic space group $P\bar{1}$ with very similar unit-cell dimensions. In **4** and **7** the $H_3O_2^-$ bridges are symmetrical with a very short O ••• H ••• O hydrogen bond at 2.496(4) Å (O ••• O) but in the ruthenium complex an asymmetric $H_3O_2^-$ bridge is present, although the O ••• O distance is within experimental error the same at 2.494(7) Å as in **4** and **7**.

The geometry of the $H_3O_2^-$ bridges in complexes **4** and **7** (Table 3) is very similar and agrees well with that reported in $[\{Co(en)_2(NO_2)\}_2(\mu\text{-}H_3O_2)][ClO_4]_3{\cdot}2\ H_2O$.[11] Only the $M\text{–}O_{H_3O_2}$ distances differ significantly in **4** [1.969(4) Å] and **7** [1.931(3) Å]. The difference of ≈0.04 Å reflects mainly the difference in ionic radii of six co-ordinate chromium(III) and low-spin cobalt(III) ions (≈0.07 Å). The same is true for the average $Co\text{–}N_{amine}$ and Co_{acac} distances which are 0.11 and 0.04 Å shorter than the corresponding bond length in **4**, respectively.

It is interesting that even the packing of the PF_6^- anions relative to the respective trication in complexes **4** and **7** is very similar. Fig. 6 gives a schematic view of the ion pairing in the solid state of **4** (top) and **7** (bottom). The most salient feature is the interaction between one PF_6^- and the $\mu\text{-}H_3O_2^-$ bridge (Table 3). Thus in **7** the F(4) ••• O(3) distance of 3.276(3) Å indicates a very weak F ••• H–O hydrogen bond. The same interaction is present in crystals of **4** and appears to be somewhat stronger because the corresponding O ••• F distance is slightly shorter at 3.135(5) Å. The same PF_6^- anion forms also two weak F ••• H–C contacts to methylene groups of the co-ordinated cyclic triamine. The second crystallographically independent PF_6^- anion does not form any significant F ••• H–X hydrogen-bonding contacts to the trication in either **4** or **7**.

It is also interesting to compare the metrical details of the two isostructural complexes **2**[4] and $[RuL(acac)(OH)]PF_6{\cdot}H_2O$.[5] The water molecule of crystallization is bound to the co-ordinated OH group *via* an O–H ••• O interaction in both cases but the corresponding O ••• O distances are at 2.66(3) Å in **2** and 2.442(8) Å in the ruthenium complex. The former hydrogen bond is thus significantly weaker than the latter. It is therefore appropriate to consider the $H_3O_2^-$ group as a terminally O-bound monodentate ligand in the ruthenium complex, but **2** contains an OH^- ligand which interacts weakly with a water molecule. This situation may be described by structures **B** and **C** which imply a short symmetrical O ••• H ••• O bond in the ruthenium and an asymmetric O–H ••• O bond in **2**.

It is unfortunate that the low diffraction quality of the crystals of complex **2** and its ruthenium analogue did not allow an unambiguous location of the hydrogen-atom positions in order to verify the above hypothesis experimentally.

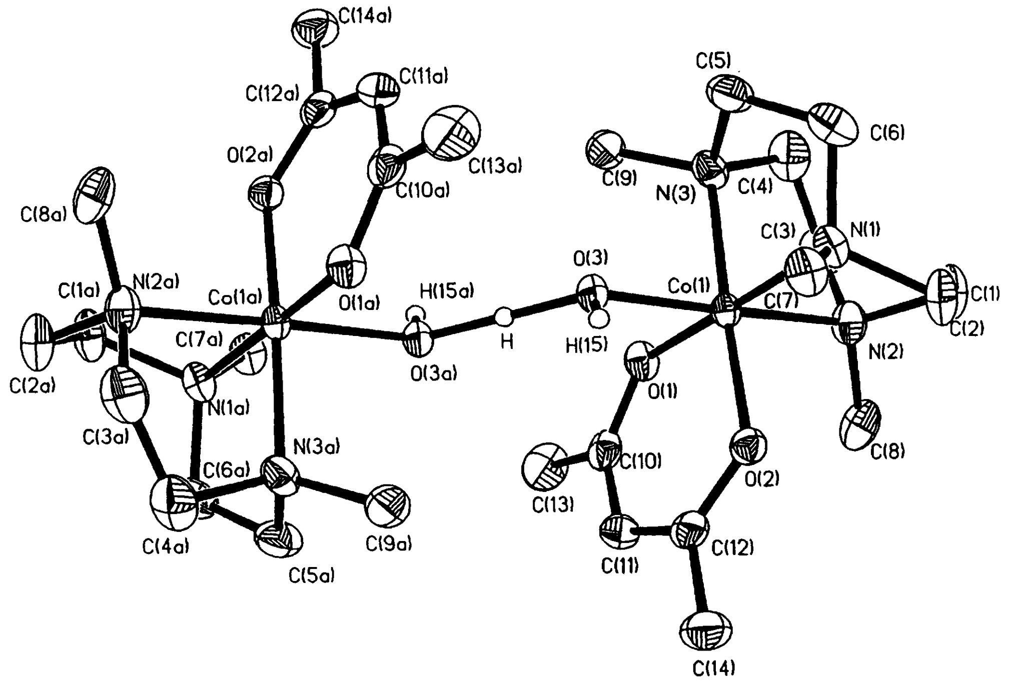

Fig. 5 Structure of the dinuclear trication $[\{CoL(acac)\}_2(\mu\text{-}H_3O_2)]^{3+}$ in crystals of complex **7**

Table 3 Intra- and inter-molecular hydrogen bonding in complex **7** and in its corresponding chromium analogue **4** (in square brackets)

O(3)–H	1.248(2) [1.248(3)]	O(3)–H(15)	0.69(4) [1.00(3)]
O(3) ••• O(3a)	2.496(4) [2.496(4)]		
		Co(1)–O(3)–H(15)	107(3) [107(3)]
		Co(1)–O(3)–H	120.3(2) [119.3(3)]
O(3)–H–O(3a)	180 (180)	H(15)–O(3)–H	112(2) [115(2)]
O(3) ••• F(4)	3.276(3) [3.135(5)]	C(4) ••• F(6)	3.046(5)

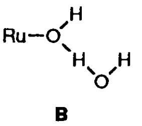

B

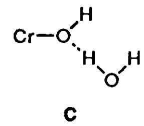

C

Discussion

The most salient feature of the present study is the remarkable quantitative solid-state transformation of dinuclear **4** at 145 °C to yield the two mononuclear complexes **5** and **6** with evolution of gaseous HF as is depicted in equation (4). It is puzzling that the analogous complex **7** does not undergo a similar reaction even at higher temperatures ($\approx$200 °C) if one considers the fact that **4** and **7** are isostructural and that even the ion pairing between the respective trication and PF_6^- anions in both structures is very similar (Fig. 6).

Since 3 equivalents of HF are formed in a single step it is natural to attempt to rationalize the reaction by assuming that the first molecule of HF is split off from one of the O–H ••• F hydrogen bonds so clearly present in the crystalline forms of complexes **4** and **7**. This would lead to the formation of the first P–O bond where the oxygen atom is co-ordinated to one chromium(III) centre. Scheme 2 shows a plausible mechanism which we would like to propose which requires least motion of atoms during the transformation. The oxygen of the P–O–Cr moiety is now less nucleophilic than in the former $H_3O_2^-$ bridge and, consequently, the central O ••• H ••• O hydrogen bond now may be asymmetric, generating an Cr–OPF_5 intermediate which is hydrogen bonded to a Cr–OH_2 species either *via* an oxygen or *via* a fluorine atom of the close by OPF_5 group. A second HF molecule can be split off intramolecularly producing thereby the second P–O bond in a $OH(O)PF_4^{2-}$ bridged dinuclear intermediate **II** which readily forms the third molecule of HF again intramolecularly, giving the dinuclear $O_2PF_3^{2-}$-bridged intermediate **III**. Finally **III** rearranges intramolecularly with formation of the thermodynamically most stable $O_2PF_2^-$ anion and the fluoro complex **5**.

In this plausible sequence of reaction steps the formation of the first HF molecule may be an unfavourable event in complex **7** because the Co–OH ••• F–PF_5 hydrogen bond is somewhat weaker than in **4**. Also, due to the shorter $Co–O_{H_3O_2}$ bonds in **7** the PF_6^- anion cannot move as closely toward the cobalt-co-ordinated oxygen atom of the $H_3O_2^-$ bridge to facilitate the subsequent rearrangements. This would be a steric argument. On the other hand, it is well established that substitution reactions at octahedral low-spin cobalt(III) ions proceed *via* a dissociative interchange mechanism, at least in solution, whereas at chromium(III) centres an associatively activated interchange mechanism seems to prevail.[12] Thus the intramolecular rearrangement **III** $\longrightarrow$ products may be kinetically more favourable for Cr^{III} than for Co^{III}.

Finally it is worth pointing out that in melts (600–800 °C) of alkali-metal polyphosphates and alkaline-metal hexafluorophosphates the sole product has been identified by Raman spectroscopy to be salts of the $O_2PF_2^-$ anion [equation (5)].[8] Thus there is a clear thermodynamic driving force for the

$$2(PO_3^-)_n + nPF_6^- \longrightarrow 3nPO_2F_2^- \qquad (5)$$

formation of $O_2PF_2^-$ from PF_6^-. This is also demonstrated by the reaction of $[M(\eta^5\text{-}C_5Me_5)Cl_2]Cl_2$ with $AgPF_6$ in acetone

Table 4 Crystallographic data for complexes **3** and **5**–**7**

	3	**5**	**6**	**7**
Formula	$C_{14}H_{30}Cl_2CrN_3O_{11}$	$C_{14}H_{28}CrF_7N_3O_2P$	$C_{14}H_{28}CrF_8N_3O_4P_2$	$C_{28}H_{59}Co_2F_{18}N_6O_6P_3$
M	538.3	484.1	568.1	1128.6
Crystal symmetry	Orthorhombic	Orthorhombic	Monoclinic	Triclinic
Space group	$P2_12_12_1$	$Pna2_1$	$P2_1/m$	$P\bar{1}$
a/Å	8.923(5)	12.788(7)	8.188(6)	10.482(2)
b/Å	13.806(8)	12.841(6)	8.980(6)	10.724(3)
c/Å	18.874(8)	12.947(8)	15.784(9)	11.479(1)
α/°				72.68(2)
β/°			99.22(5)	79.90(1)
γ/°				65.14(2)
U/Å^3	2325.1(8)	2126.0(8)	1145.6(10)	1115.9(4)
Z	4	4	2	1
F(000)	1100	1004	582	578
D_c/g cm^{-3}	1.50	1.51	1.65	1.68
Crystal size/mm	0.15 × 0.15 × 0.68	0.23 × 0.27 × 0.91	0.17 × 0.29 × 0.57	0.40 × 0.40 × 0.20
μ(Mo-Kα)/mm^{-1}	0.76	0.67	0.71	0.97
Data measured	3797	3501	3754	4435
No. unique	1609 [$I \geqslant 2.5\sigma(I)$]	1568 [$I \geqslant 2.5\sigma(I)$]	2541 [$I \geqslant 2.5\sigma(I)$]	3254 [$I \geqslant 2.0\sigma(I)$]
No. of parameters	280	253	182	425
R^a	0.055	0.066	0.075	0.037
R'^b	0.046	0.056	0.072	0.039
Weighting scheme, w^{-1}	$\sigma^2(F)$	$\sigma^2(F)$	$\sigma^2(F)$	$\sigma^2(F) + 0.0002F^2$
Largest shift/e.s.d. in final cycle	0.005	0.067	0.04	0.009
Largest peak/e Å^{-3}	0.54	0.42	0.66	0.36

^{a} $R = \Sigma(|F_o| - |F_c|)/\Sigma|F_o|$. ^{b} $R' = [\Sigma w(|F_o| - |F_c|)^2/\Sigma w(|F_o|)^2]^{\frac{1}{2}}$.

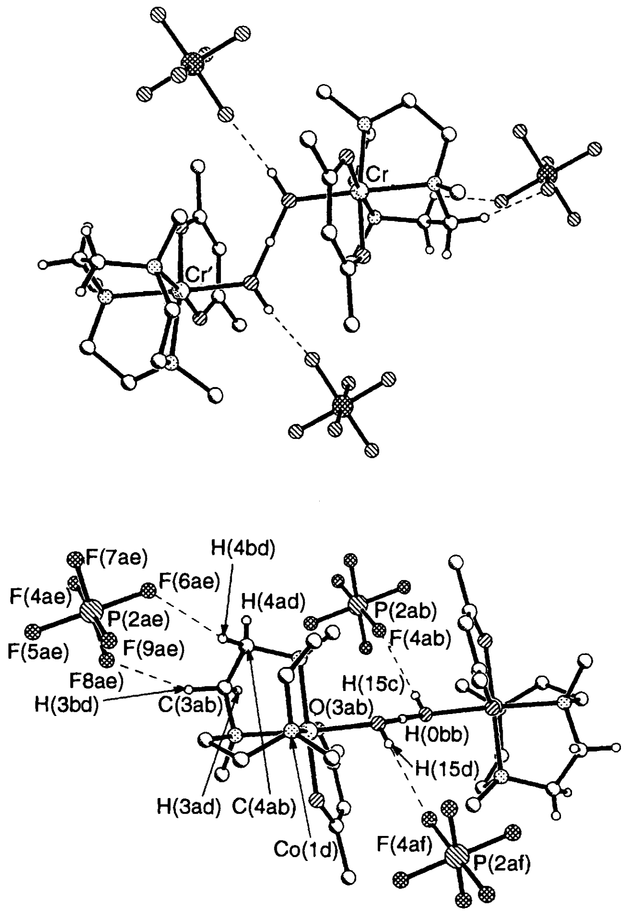

Fig. 6 Comparison of ion pairing between the PF_6^- anion and the respective trication in crystals of complexes **4** (top) and **7** (bottom)

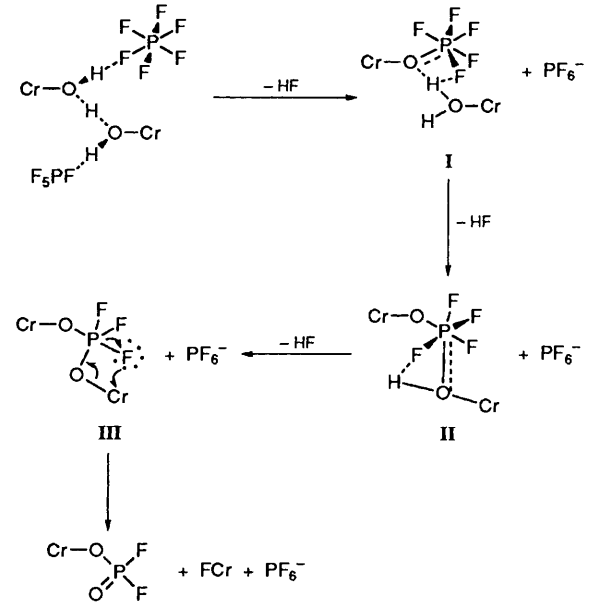

Scheme 2 Proposed reaction mechanism for reaction (4)

solution which produces $[\{M(\eta^5\text{-}C_5Me_5)\}_2(\mu\text{-}O_2PF_2)_3]PF_6$ with *O*,*O*′-bridging $O_2PF_2^-$ ligands.[13]

Experimental

Materials and Methods.—The preparations of the ligand 1,4,7-trimethyl-1,4,7-triazacyclononane[14] and the complexes $[CrLCl_3]$ **1**[15] $[CrL(acac)(OH)]PF_6{\cdot}H_2O$ **2**[4] and $[\{CrL(acac)\}_2(\mu\text{-}H_3O_2)][PF_6]_3$ **4**[4] have been described previously. All other chemicals were obtained from commercial sources and used as supplied. Infrared spectra were recorded on a Perkin-Elmer 1720 X FT spectrometer as KBr discs, electronic spectra on a Perkin-Elmer Lambda 9 UV/VIS/NIR spectrophotometer in the range 200–1500 nm. Temperature-dependent magnetic susceptibilities were measured in the range 80–298 K by using the Faraday method. Corrections for the underlying diamagnetism of solid samples were applied by use of Pascal's constants.

Table 5 Atomic coordinates (× 10^4)

Atom	x	y	z	Atom	x	y	z
Complex **3**							
Cr	408(2)	9 971(1)	1 432(1)	C(13)	−982(15)	11 861(8)	1 171(6)
N(1)	141(11)	9 437(6)	395(4)	C(14)	−242(13)	12 412(9)	1 130(7)
N(2)	−1 159(11)	8 906(7)	1 714(5)	O(1)	1 924(9)	10 885(6)	1 165(4)
N(3)	1 944(10)	8 826(7)	1 550(5)	O(2)	−1 154(8)	10 943(5)	1 319(4)
C(1)	−1 154(14)	8 726(10)	378(7)	O(3)	784(9)	10 431(5)	2 459(3)
C(2)	−2 026(14)	8 767(10)	1 052(7)	Cl(1)	−5 376(4)	11 360(2)	3 013(1)
C(3)	−341(17)	7 989(9)	1 905(7)	O(11)	−5 137(10)	11 891(5)	3 644(3)
C(4)	1 243(15)	8 106(10)	2 019(8)	O(12)	−6 820(10)	11 531(8)	2 757(6)
C(5)	2 162(15)	8 334(10)	835(7)	O(13)	−5 288(14)	10 346(6)	3 142(4)
C(6)	1 585(13)	8 950(10)	233(7)	O(14)	−4 302(13)	11 628(9)	2 520(5)
C(7)	−122(15)	10 226(7)	−128(4)	Cl(2)	−270(5)	10 299(2)	4 293(2)
C(8)	−2 223(14)	9 239(9)	2 256(6)	O(21)	1 042(11)	9 881(9)	4 012(7)
C(9)	3 409(12)	9 136(9)	1 814(6)	O(22)	39(11)	11 162(5)	4 675(5)
C(10)	3 215(12)	12 376(9)	936(7)	O(23)	−944(15)	9 628(7)	4 749(6)
C(11)	1 784(15)	11 791(10)	1 071(6)	O(24)	−1 119(15)	10 546(10)	3 683(6)
C(12)	406(17)	12 297(7)	1 085(6)				
Complex **5**							
Cr	1 075(1)	8 577(2)	5 921	O(2)	1 698(7)	9 155(7)	7 210(7)
N(1)	−298(7)	9 484(7)	6 109(11)	O(3)	1 734(6)	9 657(7)	5 116(7)
N(2)	300(9)	7 953(9)	4 687(11)	C(10)	3 011(11)	9 846(12)	8 256(12)
N(3)	237(9)	7 470(10)	6 798(11)	C(11)	2 518(9)	9 733(10)	7 212(11)
C(1)	−907(16)	9 347(16)	5 124(16)	C(12)	2 918(11)	10 220(12)	6 331(14)
C(2)	−605(14)	8 638(18)	4 435(13)	C(13)	2 518(11)	10 239(11)	5 354(13)
C(3)	−17(19)	6 943(15)	4 983(16)	C(14)	2 938(11)	10 893(12)	4 554(13)
C(4)	−151(13)	6 733(11)	6 055(21)	P	1 378(4)	3 609(4)	6 451(5)
C(5)	−614(18)	8 091(19)	7 255(17)	F(11)	527(9)	4 138(11)	7 098(13)
C(6)	−935(19)	8 949(21)	6 848(25)	F(12)	1 459(13)	2 676(10)	7 147(13)
C(7)	−128(9)	10 582(9)	6 344(12)	F(13)	2 129(11)	4 185(18)	7 075(23)
C(8)	938(10)	7 817(11)	3 735(11)	F(14)	1 196(21)	4 487(13)	5 697(12)
C(9)	883(11)	6 922(12)	7 556(12)	F(15)	2 240(13)	3 163(12)	5 863(22)
F(1)	2 194(4)	7 667(5)	5 727(7)	F(16)	629(21)	3 020(15)	5 860(25)
Complex **6**							
Cr	4 253(1)	2 500	2 282(1)	P(2)	4 788(4)	2 500	233(1)
N(1)	6 070(5)	936(5)	2 758(3)	O(11)	5 018(7)	2 500	1 165(3)
N(2)	3 765(7)	2 500	3 547(3)	O(12)	6 239(9)	2 500	−172(4)
C(1)	5 665(10)	364(8)	3 582(5)	F(13)	3 666(6)	1 201(6)	−82(3)
C(2)	4 527(9)	1 140(9)	3 955(4)	P(1)	705(3)	7 500	3 981(1)
C(3)	7 689(7)	1 726(7)	2 885(6)	F(14)	2 555(9)	7 500	3 955(9)
C(4)	6 169(8)	−327(7)	2 178(4)	F(15)	293(20)	−3 708(13)	3 316(7)
C(5)	1 969(9)	2 500	3 603(6)	F(16)	−1 167(10)	7 500	4 037(6)
O(1)	2 640(4)	969(4)	1 934(2)	F(17)	1 308(18)	−1 262(12)	4 637(7)
C(6)	392(7)	−346(8)	1 168(4)	F(18)	674(27)	7 500	4 922(10)
C(7)	1 229(6)	1 129(6)	1 434(3)	F(19)	550(36)	9 241(21)	3 920(27)
C(8)	552(9)	2 500	1 173(5)	F(20)	687(72)	7 500	3 078(15)
Complex **7**							
Co(1)	1 711(1)	3 045(1)	1 867(1)	C(12)	3 664(3)	3 215(4)	−132(3)
O(1)	1 692(2)	4 886(2)	1 495(2)	C(13)	2 160(5)	6 900(5)	463(6)
O(2)	3 221(2)	2 403(2)	742(2)	C(14)	4 651(4)	2 502(5)	−1 053(4)
O(3)	432(2)	3 728(2)	584(2)	P(1)	5 000	5 000	5 000
N(1)	1 744(3)	1 084(2)	2 394(2)	F(1)	4 395(11)	5 346(9)	6 264(5)
N(2)	2 944(3)	2 460(3)	3 217(2)	F(2)	4 917(12)	3 484(9)	5 525(10)
N(3)	93(3)	3 525(3)	3 073(2)	F(3)	3 505(8)	5 602(13)	4 547(9)
C(1)	3 129(5)	211(4)	2 970(4)	F(1a)	6 134(26)	3 842(40)	4 445(41)
C(2)	3 335(5)	921(4)	3 812(4)	F(2a)	5 877(54)	4 393(46)	6 222(23)
C(3)	2 012(5)	3 367(5)	4 086(3)	F(3a)	4 173(30)	4 150(34)	5 387(23)
C(4)	620(5)	3 303(5)	4 271(3)	P(2)	2 031(1)	730(1)	7 793(1)
C(5)	−569(4)	2 496(4)	3 148(4)	F(4)	1 746(3)	1 867(2)	8 539(2)
C(6)	522(5)	1 058(4)	3 283(3)	F(5)	3 318(2)	−345(2)	8 614(2)
C(7)	1 705(4)	506(4)	1 373(3)	F(6)	748(3)	1 814(3)	6 985(2)
C(8)	4 238(5)	2 765(5)	2 847(4)	F(7)	1 008(3)	156(3)	8 740(2)
C(9)	−988(4)	4 989(4)	2 700(4)	F(8)	3 063(3)	1 319(4)	6 860(2)
C(10)	2 381(4)	5 385(3)	584(3)	F(9)	2 314(3)	−378(3)	7 045(3)
C(11)	3 280(4)	4 648(4)	−240(3)				

The FAB mass spectra were measured on a VG AutoSpec Fisons instrument by LSIMS (liquid secondary ion mass spectrometry) with *m*-nitrobenzyl alcohol as a matrix.

Preparation of Complexes.—$[CrL(acac)(OH_2)][ClO_4]_2$ **3**. A mixture of complex **1** (1.50 g, 4.6 mmol) and sodium pentane-2,4-dionate (1.5 g, 14.8 mmol) in water was heated to 75 °C with stirring until a clear deep red solution was obtained. It was adjusted to pH 1 by dropwise addition of concentrated $HClO_4$. Addition of $NaClO_4$ (1.5 g) initiated precipitation of red crystals of complex **3** which were filtered off. Yield: 2.1 g (85%) (Found: C, 31.6; H, 5.8; N, 7.6. Calc. for $C_{14}H_{30}Cl_2CrN_3O_{11}$: C, 31.2; H, 5.6; N, 7.8%).

$[CrL(acac)F]PF_6$ **5**. A solid sample of complex **4** (1.0 g, 0.9 mmol) was heated *in vacuo* at 160 °C for 4 h after which time the cooled residue was dissolved in water (10 cm^3) and the pH adjusted to 9 with NaOH. After standing in an open vessel for 2–3 d red needles crystallized which were filtered off. Yield: 0.15 g (33% with respect to the starting material **4**). Recrystallization from alkaline aqueous solution produced single crystals suitable for X-ray crystallography (Found: C, 33.8; H, 5.6; N, 8.2. Calc. for $C_{14}H_{28}CrF_7N_3OP$: C, 34.5; H, 5.8; N, 8.6%).

$[CrL(acac)(O_2PF_2)]PF_6$ **6**. Treatment of complex **4** in the same fashion as described above for **5** and dissolution of the solid residue in water (10 cm^3) with adjustment of the pH to 5 by using aqueous HPF_6 produced pink-red microcrystals of **6** after 2–3 d of standing in an open vessel. Yield: 0.18 g (33% with respect to **4**). Recrystallization from an acidic aqueous solution (pH 5) produced single crystals suitable for X-ray crystallography (Found: C, 31.0; H, 5.3; N, 7.6. Calc. for $C_{14}H_{28}CrF_8N_3O_4P_2$: C, 29.6; H, 5.0; N, 7.4%).

$[CoLCl_3]\cdot H_2O$. To a solution of $Na_3[Co(NO_2)_6]$ (10.0 g, 24.8 mmol) in water (15 cm^3) was added a solution of L (3.4 g, 20 mmol) in methanol (15 cm^3). The red-brown reaction mixture was stirred at 60 °C for 1 h. Upon cooling to 2 °C a yellow precipitate of $[CoL(NO_2)_3]$ formed which was filtered off. Yield: 7.1 g (96%). To solid $[CoL(NO_2)_3]$ (7.0 g, 19.1 mmol) was added in small amounts concentrated HCl (35 cm^3). The mixture was heated to 70 °C with stirring until the evolution of gaseous NO_2 ceased. Upon cooling a green precipitate was obtained which was filtered off. Yield: 5.9 g (92%). This material has not been further characterized but was used as prepared for the synthesis of complex **7**.

$[\{CoL(acac)\}_2(\mu\text{-}H_3O_2)][PF_6]_3$ **7**. A suspension of $[CoLCl_3]\cdot H_2O$ (4.0 g, 11.9 mmol) and sodium pentane-2,4-dionate (2.0 g, 16.4 mmol) in water (40 cm^3) was heated to 70 °C until a clear red solution was obtained. It was adjusted to pH 6 by addition of aqueous HPF_6. Addition of $NaPF_6$ (2.0 g) initiated the precipitation of deep red violet microcrystals which were filtered off. Yield: 4.9 g (37%) (Found: C, 29.5; H, 5.3; N, 7.2. Calc. for $C_{28}H_{59}Co_2F_{18}N_6O_6P_3$: C, 29.7; H, 5.4; N, 7.4%).

Crystal Structure Analyses.—Table 4 summarizes the relevant data for the crystal-structure determinations. Final atom coordinates are given in Table 5 for the four structures **3** and **5**–**7**. Intensity data were collected on an AED II (Siemens) (**3**, **5**), a Syntex R3 (**6**), or a Siemens P4 (**7**) diffractometer by using graphite-monochromated Mo-Kα X-radiation (λ = 0.710 73 Å) at ambient temperature and were corrected for Lorentz, polarization and absorption effects (ψ scans for **3**, **5** and **6**) in the usual manner. The structures were solved by conventional Patterson and Fourier difference methods by using the SHELXTL-PLUS (personal computer version) program package.[16] The function minimized during full-matrix least-squares refinement was $\Sigma w(|F_o| - |F_c|)^2$: Neutral-atom scattering factors and anomalous-dispersion corrections for non-hydrogen atoms were taken from ref. 17. The positions of the methine, methylene and methyl hydrogen atoms in complexes **3**, **5** and **6** were calculated and included with fixed isotropic thermal parameters. The hydrogen atoms of the coordinated water molecule in **3** have not been located. For **7** all hydrogen atoms were located in the final Fourier difference map and were refined with isotropic thermal parameters as variable. The absolute configuration of **3** was checked by fully refining the structure in both configurations. For **5** the absolute configuration was also checked but it has not been possible unambiguously to decide which is the correct one. The PF_6^- anion in **6** and one PF_6^- in **7** were found to be disordered. In both species this disorder was successfully modelled by a split-atom model.

Additional material available from the Cambridge Crystallographic Data Centre comprises H-atom coordinates, thermal parameters and remaining bond lengths and angles.

Acknowledgements

We thank the Fonds der chemischen Industrie for financial support.

References

1 M. Ardon and A. Bino, *Struct. Bonding (Berlin)*, 1987, **65**, 1.

2 K. Michelsen, *Acta Chem. Scand., Ser. A*, 1972, **26**, 1517.

3 F. Galsbøl, S. Larsen, B. Rasmussen and J. Springborg, *Inorg. Chem.*, 1986, **25**, 290.

4 U. Bossek, K. Wieghardt, B. Nuber and J. Weiss, *Angew. Chem.*, 1990, **102**, 1093; *Angew. Chem., Int. Ed. Engl.*, 1990, **29**, 1055.

5 R. Schneider, T. Weyhermüller, K. Wieghardt and B. Nuber, *Inorg. Chem.*, 1993, **32**, 4925.

6 K. Wieghardt, W. Schmidt, B. Nuber and J. Weiss, *Chem. Ber.*, 1979, **112**, 2220.

7 (*a*) M. F. A. Dove, R. C. Hibbert and N. Logan, *J. Chem. Soc., Dalton Trans.*, 1985, 707; (*b*) S. D. Brown, L. M. Emme and G. L. Gard, *J. Inorg. Nucl. Chem.*, 1975, **37**, 2557.

8 K. Bühler and W. Bues, *Z. Anorg. Allg. Chem.*, 1961, **308**, 62.

9 K. Dehnicke and A.-F. Shihada, *Struct. Bonding (Berlin)*, 1976, **28**, 52.

10 B. Morosin, *Acta Crystallogr.*, 1965, **19**, 131.

11 M. Ardon, A. Bino and W. G. Jackson, *Polyhedron*, 1987, **6**, 181.

12 R. G. Wilkins, *Kinetics and Mechanism of Reactions of Transition Metal Complexes*, VCH, Weinheim, 1991.

13 S. J. Thompson, P. M. Bailey, C. White and P. M. Maitlis, *Angew. Chem.*, 1976, **88**, 506; *Angew. Chem., Int. Ed. Engl.*, 1976, **15**, 490.

14 K. Wieghardt, P. Chaudhuri, B. Nuber and J. Weiss, *Inorg. Chem.*, 1982, **21**, 3086.

15 P. Chaudhuri, M. Winter, H. J. Küppers, K. Wieghardt, B. Nuber and J. Weiss, *Inorg. Chem.*, 1987, **26**, 3302.

16 G. M. Sheldrick, SHELXTL-PLUS, Universität Göttingen, 1990.

17 *International Tables for X-Ray Crystallography*, Kynoch Press, Birmingham, 1974, vol. 4, pp. 99, 149.

Received 4*th February* 1994; *Paper* 4/00695J